Presented at the ASNE Advanced Propulsion Confernece, Arlington, VA, Oct 30-31 2006

Crashback Simulations of a Notional Destroyer-Class All-Electric Ship

M. Andrus, S. Woodruff, M. Steurer, and W. Ren

***Abstract*—Crashback is one of the most dramatic maneuvers a naval combatant can perform. Propulsion power can go from full ahead to full astern in minutes and the rate of change of power itself changes dramatically during this period. The integrated power system of an all-electric ship can experience unfortunate electrical disturbances and even system-wide instability.**

This paper investigates the dynamics of crashback maneuvers on IPS performance. A detailed description of the crashback maneuver is given with emphasis on the problems posed for motor control during each phase of the maneuver. A discussion of the possibilities for drive controller optimization are then presented. A notional destroyer-class all-electric ship simulation capability developed on the Real Time Digital Simulator (RTDS) is described. Finally, simulation results for crashback simulations performed under varying conditions are given with the propulsion motor drives operating under speed control and then power control.

***Index Terms*—integrated power system, IPS, real-time digital simulator, RTDS, crashback, power control, speed control, simulation, modeling.**

I. INTRODUCTION

The crashback maneuver involves slowing, stopping and reversing the direction of a ship as rapidly as possible. Often this is done to avoid an obstacle. As one of the more dramatic maneuvers a ship can perform, the crashback is an important maneuver to analyze, both in order to gain an understanding of the basic principles involved, and to improve crashback performance during the design of specific ships. Large-scale simulation capabilities provide a critical tool for analyzing crashback and other maneuvers of the all-electric ship. Simulation of the electrical generation, propulsion and power distribution systems can permit accurate and detailed assessments of maneuver performance and of the interactions between different parts of the system during the maneuver. Thus, disturbances in the distribution system due to the maneuver can be quantified and assessed, as well as any effects ship loads may have on destabilizing or otherwise degrading ship-system performance during the maneuver.

The crashback has been implemented for many types of ships for many decades and discussions of the maneuver are nothing new. Chase, et. al. [1] and Crane, et. al. [2] developed empirical models for estimating the time and distance required to bring a ship moving in the forward direction to a full stop (i.e., *time-to-stop* and *head reach* respectively). Lecourt [3] performed computer simulations of the crashback maneuver for an electric-drive ship. In the present paper, simulations are presented of the performance of a complete, notional destroyer-class, all-electric ship integrated power system (IPS) in the crashback using a number of controller architectures and settings. The opening sections review and analyze the crashback maneuver, with particular emphasis on the possibilities for optimization for the electric ship. It is hoped that this review will be of particular use to power-system practitioners not so familiar with the naval-architecture aspects of electric-ship work. Two control schemes for the crashback maneuver, a power-control scheme and a speed-control scheme, are implemented in a simulation of a notional destroyer-class electric ship. Results of simulations of the crashback maneuver, showing ship performance and the nature of disturbances caused throughout the ship system by the maneuver are examined for a variety of scenarios and controller specifications. This type of investigation permits trends in system behavior during the crashback to be studied, such as the effect of changing the maximum permitted regeneration. Based on large-scale simulations, such investigations will become increasingly common as a way for electric-ship researchers and designers to build an understanding of electric-ship characteristics, particularly in the absence of full-size tests.

The simulations reported here were carried out on the Center for Advanced Power System's (CAPS') 14-rack real-time digital simulator (RTDS) (Kuffel, et al., [4]). CAPS has developed a nine-rack simulation of the

electrical system of a notional destroyer-class electric ship (Andrus [5]), which includes detailed modeling of the gas-turbine generators, the motors and drives and a five-zone power distribution system.

In the following section, a detailed description of the crashback maneuver is given. The problems posed by control of each phase of the maneuver and the possibilities for optimization are discussed. An overview of the RTDS E-ship model and its propulsion motor control follows. Then, results are provided from E-ship model crashback simulations under varying conditions. Finally, conclusions are drawn from the results.

A companion paper (Ren, et al., [6]) describes hardware-in-the-loop experiments of the crashback maneuver performed at CAPS employing the power control described here, and using CAPS' 20 hp and 2.5 MW motor sets.

II. CRASHBACK CONTROL AND OPTIMIZATION

The crashback maneuver may be divided into four phases, as shown in Figure 1. In the first phase, the propulsion motor speed and power are reduced until the hydrodynamic load torque decreases to zero and the propulsion motors begin to generate, rather than consume, power. In the second phase, this regeneration condition continues until the ship has slowed sufficiently that the propeller speed may be reduced to zero without exceeding the regeneration limits of the system.

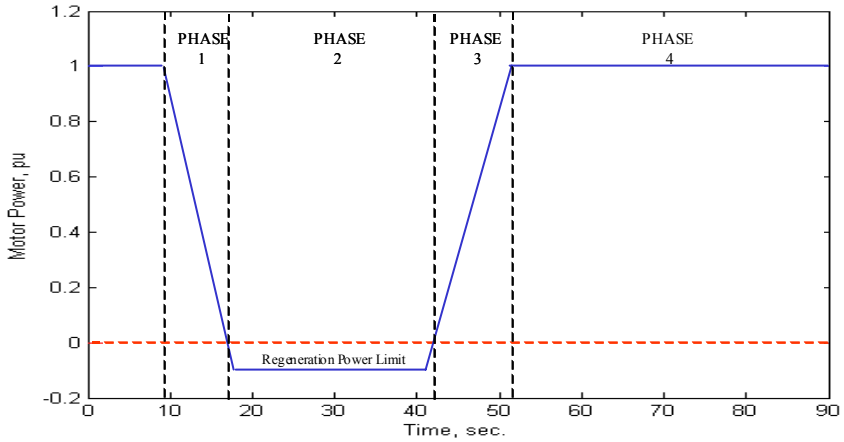

Power Control – Motor Power

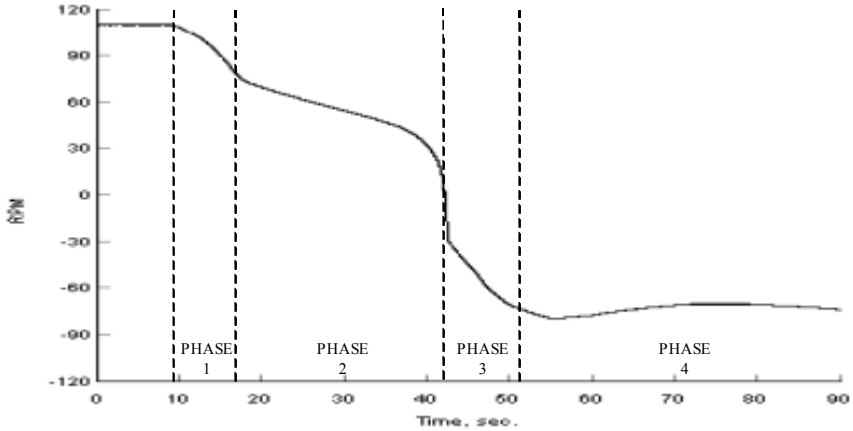

Power Control – Motor Speed

Figure 1. Power Crashback Profile

The third phase involves the acceleration of the propeller in the negative direction until the desired speed or power is achieved in reverse. Finally, in the fourth phase, the propulsion system remains almost in a steady state, with the propeller speed changing only slightly to maintain the desired level of power as the ship slows down. Each of the four phases is limited by different physical and system factors, so each represents a different problem for control and optimization.

1. Phase One

The goal of the first phase of the maneuver is to reduce the propeller speed as rapidly as possible until the load torque changes sign and the system goes into regeneration. This is because the overall goal of any optimization with regard to the crashback maneuver is, of course, to minimize the time required stopping the ship. Barring any problems with over-stressing the drive shafts mechanically during the deceleration, the limiting factor here will be the ability of the gas-turbine generators to shed the propulsion motor load. This may be handled by simply establishing a maximum power ramp rate (or speed ramp rate, in the case of speed control) that is certain to be within system limits and controlling the motors so these rate limits are never exceeded. This is the approach employed in the present generic power control. Alternatively, the motors might be controlled so that the instantaneous rate of change of the system is always the maximum the gas-turbine generators can safely support at that time. This latter approach would lead to performance improvements if the single fixed limit is unduly restrictive during much of the maneuver.

2. Phase Two

The second phase of the crashback maneuver begins when the torque changes sign and ends when the propeller speed goes through zero. In this regeneration period, the propeller rotation is positive, the load torque is negative and the propulsion motors generate power. The level of permissible regeneration is determined by system considerations: the system loads available to take up power if the motor drives are regenerative, the capacity of braking resistors in the system, etc. The regeneration period must be continued until the ship slows sufficiently that the propeller speed can drop to zero without causing more power to be regenerated than the system can handle. Once the regeneration limit has been fixed, the length of the regeneration period is determined entirely by the hydrodynamic load characteristics.

Figure 2 illustrates the relationship between propeller advance ratio (υ) and torque coefficient (Cq) for the propellers employed on a destroyer-class Navy ship. The upper and lower curves correspond to negative and positive ship speed, respectively. Similarly, curve data to the left and right of center correlate to negative and positive propeller speed, respectively.

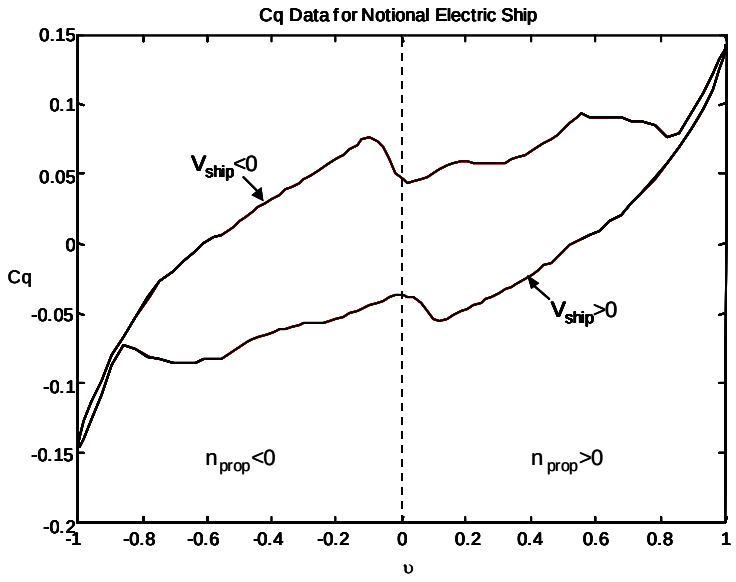

Figure 2. Propeller Torque Coefficient

The hydrodynamic load is such that the torque (and power) increase with increasing propeller speed for most of the positive range of propeller speeds. The exception to this rule is near zero speed, where the power reaches a maximum regenerative (i.e., negative) value at an advance ratio around 0.1 to 0.2. Advance ratio is calculated from the velocity of ship advance (V_a), the propeller speed (*n, i.e.,* n_{prop}), and the propeller diameter (D) by:

$$\upsilon = \frac{nD}{\sqrt{V_a^{\,2} + (nD)^2}} \tag{1}$$

where V_a is related to ship velocity by the Taylor wake fraction, i.e., $V_a = (1\text{-}w_T)V_{ship}$.

Propulsion motor power as a function of υ is given by:

$$P = C_P(\upsilon)\rho\left(\frac{D^3}{\eta_r}\right)(V_a^{\,2} + (nD)^2) \tag{2}$$

where ρ is the density of salt water and η_r is the relative rotational efficiency. $C_P(\upsilon)$ is a propeller power coefficient which is related to the more frequently used propeller torque coefficient by the equation $C_P(\upsilon) = \upsilon C_Q(\upsilon)$. Let the value of υ at the point of maximum regenerative power be $\upsilon_{rmax,}$ and the corresponding value of the power coefficient be C_{Prmax}. At any given ship speed V_a, the propeller speed for maximum regeneration, n_{rmax}, can be computed using the value $\upsilon_{rmax.}$. The maximum regenerative power, P_{rmax}, can be computed using the value C_{Prmax}. If the magnitude of P_{rmax} exceeds the regeneration limit imposed by the system, the controller is forced to wait for the ship to slow down before the propeller can be further slowed and reversed. The values of C_{Prmax} and υ_{rmax} thus determine how long the second, regeneration phase of the maneuver lasts. The ship speed at which propeller reversal can occur may be determined using the system regeneration limit and these two values.

This last consideration places a hard limit on the first two phases of the crashback maneuver. The propeller can be reversed only when the ship speed is reduced to a value that makes P_{rmax} equal to or less than (in magnitude) the regeneration limit. Thus, the goal of the first two phases is to reduce the ship speed as quickly as possible. This is achieved by reducing the forward thrust as quickly as the system will permit, which in turn implies that the propeller speed, or the motor power, should be reduced as fast as possible. (The thrust, torque and power curves are all monotonic functions of speed in the region relevant for this part of the maneuver, implying that minimum speed, torque and power are equivalent.) With power control, this goal is approximated by maintaining a fixed power ramp in phase one and constant power at the regeneration limit in phase two. With speed control, a fixed speed ramp is used in phase one and the ramp override is used to maintain constant power regeneration in phase two.

When the ship has slowed sufficiently, the propeller may be slowed to zero speed, reversed and accelerated in the negative direction, beginning the third phase of the maneuver. This phase is not explicitly initiated by the controller (that is, there is no need to explicitly compute the ship speed at which reversal may occur and monitor the ship speed to see when this speed has been reached) because of the change in the system's stability properties caused by passing through the maximum power point.

In ordinary forward motion, with the propellers providing positive thrust, the torque increases with increasing speed. This causes the hydrodynamic propeller load to be stabilizing, in the sense that a disturbance to the system that causes an increase in speed will cause the load torque to increase and, other things being equal, the speed will be reduced. Similarly, a disturbance causing a decrease in speed will decrease the load torque, permitting the speed to increase.

This stable behavior is maintained even when the torque changes direction as the speed is decreased and the system goes into regeneration, until the maximum regeneration point is reached. At that point, the rate of change of torque with speed is zero, and beyond that point (that is, at lower speeds), the speed-torque

relationship is reversed. The load is now de-stabilizing, but only until the propeller reverses direction, where the slope of the speed-torque curve goes back to positive and the original state of affairs is restored.

When the ship speed is low enough, the specified level of regeneration becomes impossible to maintain, the power controller will change the torque (or current) reference in a futile effort to maintain the requested (regenerative) power. If the result is a propeller-speed increase (in the direction of a stabilizing load), the load will tend to decrease the propeller speed, pushing the system back towards the maximum regeneration point. If the controller pushes the system to decrease the propeller speed, the destabilizing load will push it further in that direction, until the propeller reverses direction and stable operation becomes possible again. Thus, the system automatically leaves the regenerative mode and reverses the propeller without explicit action by the controller. Once propeller reversal takes place, the power-control loop resumes control after a second or two. In speed control, the system behaves similarly.

3. Phases Three and Four

In the third phase of the crashback maneuver, the system comes out of regeneration and the propeller reverses and increases speed (in the negative direction) until the requested level of reverse speed/power is reached. As explained above, the power controller regains control after the propeller reverses. The controller then ramps up to the operator-specified reverse power level, or, in the case of speed control, to the operator-specified reverse speed.

The fourth and final phase of the maneuver sees the ship continuing to decelerate until it reaches zero speed. The time required to bring the ship to zero speed, and the distance it covers before it stops, are common measurements of crashback performance. If the maneuver is continued beyond the zero-speed point, the ship eventually reaches a steady-state negative speed. During this fourth phase, very little control action is required to maintain the requested level of reverse power. The nature of the hydrodynamic load power curve is such that a momentary reduction in propeller speed is necessary to pass over a load-power maximum without exceeding the power limit just after maximum reverse power is reached. This behavior is seen when speed control is used as well. From that point on, constant power is maintained by the power control by gradually increasing the propeller speed as the (reverse) ship speed increases. In speed control, constant propeller speed is maintained until the steady state is reached.

III. RTDS E-SHIP MODEL OVERVIEW

The simulation capability used in this study is based on a concept for the IPS of a notional destroyer developed by the Syntek corporation under contract to the Office of Naval Research [7] and [8]. This concept is depicted in Figure 3. It involves a power generation system, a propulsion system, and a DC zonal electric distribution system (DC ZEDS).

A 13.8 kV medium voltage (MV) ring bus is supplied by two 36 MW main gas turbine, synchronous generators (i.e., MTG 1 and MTG 2), and two 4 MW auxiliary gas turbine generators (i.e., ATG 1 and ATG 2). The MV subsystem supplies two 36.5 MW propulsion motors, a 3 MW shipboard radar, and three AC-DC power conversion modules (i.e., PCM 4s) that rectify 13.8 kV AC to 1 kV DC for powering port and starboard DC buses. The longitudinal DC buses feed 1 kV DC power to load centers in five zonal regions along the ship.

Figure 4 shows that at the zonal level, port and starboard DC-DC power conversion modules (i.e., PCM 1s) step the DC bus voltage from 1 kV down to 800 V. These converters simultaneously feed an 800VDC bus through auctioneering diodes, which perform continuous current sharing between the two PCM 1s. Some DC load equipment operates directly from this bus. AC loads are supplied through a DC-AC inverter (i.e., PCM 2) that converts 800 VDC to 120/208 VAC or 450 VAC.

The CAPS E-ship model implements this notional IPS concept through the use of 116 parallel digital signal processors (DSPs) and 11 RISC processors on nine racks of the RTDS. The electrical network is defined by 345 nodes and includes representation of all AC circuit breakers and DC disconnect switches. The simulation runs in real-time with a fixed time step of 85 μs.

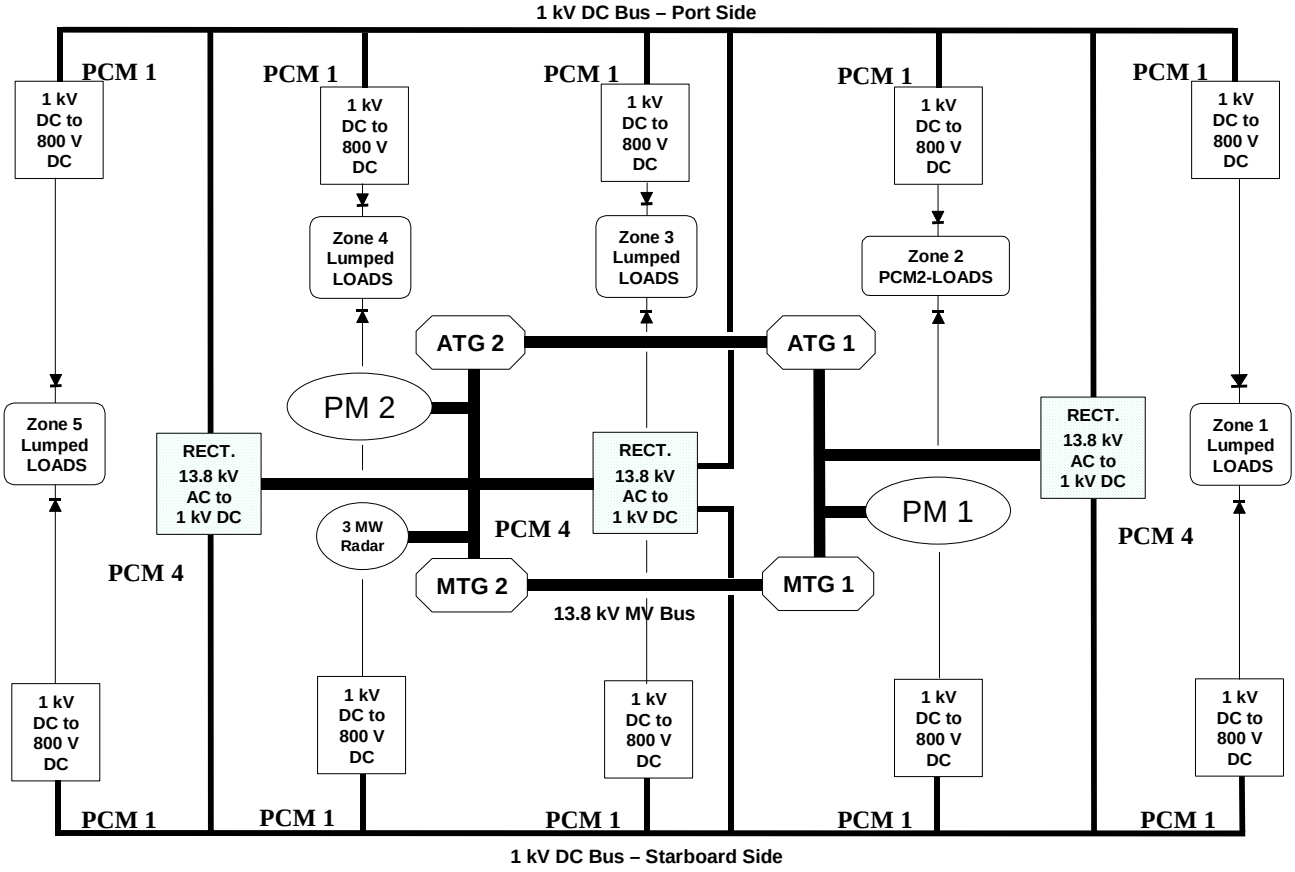

Figure 3. RTDS IPS DCZEDS Model

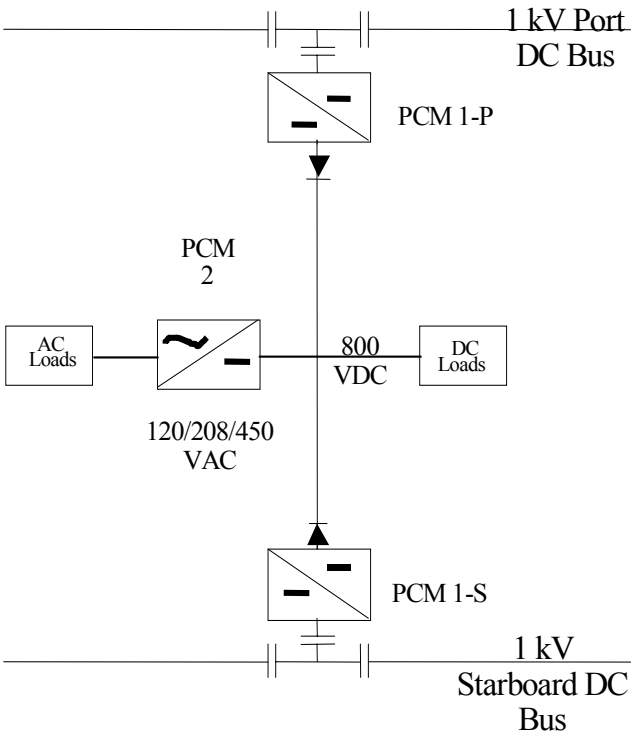

Figure 4. DC Zone Architecture

A DQ-axis synchronous machine model with a voltage regulator/exciter, prime mover, and governor represents the main and auxiliary generators. An aero-derivative gas turbine model is employed that includes details of the governor, combustion chamber, and exhaust gas temperature measurement time constants. The voltage regulator is a generic model employing PI control. A load sharing routine monitors the real and reactive powers supplied by each generator and provides control signals to equally divide the loads between connected generators as a fraction of each generator's capacity.

A DQ-axis induction motor model represents the propulsion motors. The motor drives are back-to-back, two-level, GTO bridges with front-end PWM control switching at 1 kHz. The motors employ vector control and active damping is used in the drive front-end controls to complement passive filtering in minimizing drive harmonic distortion.

All power conversion modules are modeled as ideal switching devices. PCM 4 rectifiers are 12-pulse thyristor-driven modules with PI voltage control. PCM 1 DC buck converters switch at 1 kHz and employ proportional-integral (PI) voltage control. PCM 2 inverters are sinusoidal PWM GTO modules with current and voltage control. They execute on a special, high-speed RISC processor that runs at time steps of less than 2 μs.

Ship's service loads are represented in the RTDS E-ship model as lumped load categories at the 800 VDC bus level based on [8]. Figure 5 shows a typical load configuration for Zone 1.

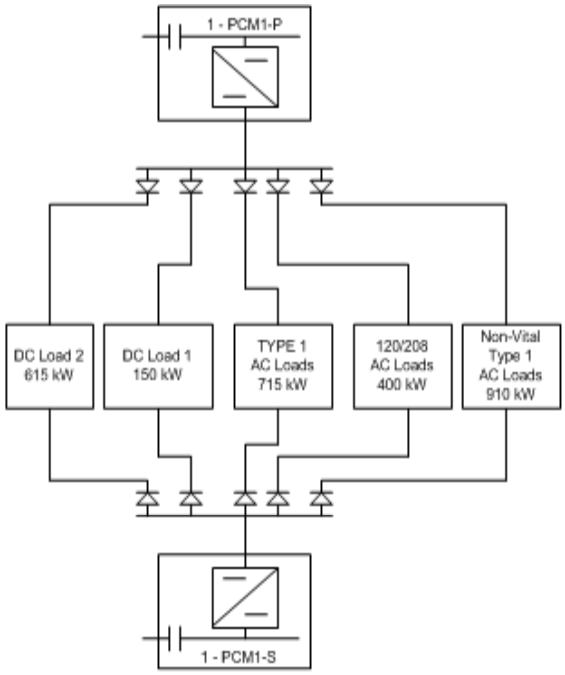

Figure 5. Zonal Load Configuration

The hydrodynamic torque loading of the propulsion motors and the thrust exerted on the ship by the propellers are modeled according to Lecourt's formulation [3]. Empirical data for destroyer-class propeller torque coefficient, thrust coefficient and ship resistance were extracted from [7]. These data permit predictions of the time required to bring a ship to a full stop, i.e., *head reach*, and the *time-to-stop* that account for the complex dynamics of the propeller torque and thrust characteristics over the full range of propulsion motor and ship speeds. Validation of the RTDS E-ship hydrodynamic model can be accomplished in part by comparing the model's predictions of head reach and time-to-stop with empirical estimates for these variables derived from techniques developed by Crane, et. al., [2].

Crane, et. al., [2] defines the head reach as:

$$\text{Head Reach, i.e., HR, in feet} = D(\text{m-}X_{\dot{u}})\, V_o^2 /\ 2R_o \tag{3}$$

where:

D = dynamic potential, i.e., a dimensionless ratio which relates effective energy expended to the loss of kinetic energy of the ship.

m = mass of the ship,

$X_{\dot{u}}$ = added mass in the *x*-direction,

V_o = speed of the ship in the forward direction at the start of the maneuver, and

R_o = ship resistance at the ship speed of V_o, .

The dynamic potential is expressed by $D = D_i + \delta D$, where D_i is the value of dynamic potential for a constant astern thrust instantaneously applied. It is given in Crane, et. al., [2] by empirically-derived curves of $R_o/\ T_1$ vs. D_i, where T_1 is the value of astern thrust at the point where the ship is dead in the water. The term δD is a correction to D that takes into account the fact that it takes finite time for the astern thrust to develop. Values of δD are obtained from empirically-derived curves that are functions of T_1/R_o and another dimensionless ratio termed dynamic impulse at the time (t_r) when the motor throttle is open in the astern direction, i.e., τ_r. The expression m-$X_{\dot{u}}$ is equal to 75 times the ship displacement in long tons.

Dynamic impulse is the impulse supplied by the ship's resistance up until the loss of momentum of the ship. At time t_r, it is given by the formula:

$$\tau_r = R_o\, t_r /(\text{m-}X_{\dot{u}})\, V_o \tag{4}$$

The time-to-stop (TS) is given in Crane, et. al., [2] by:

$$\text{TS, in seconds} = \tau\ (\text{m-}X_{\dot{u}})\, V_o /R_o \tag{5}$$

where τ is expressed by $\tau = \tau_i + \delta\tau$. The term τ_i is the dynamic impulse for a constant astern thrust instantaneously applied. It is given in Crane, et. al., [2] by empirically-derived curves of $R_o/\ T_1$ vs. τ_i. The fact that it takes finite time for the astern thrust to develop is accounted for by the variable $\delta\tau$, which is obtained from empirically-derived curves of T_1 /R_o vs. τ_r.

Using these equations, head reach and time-to-stop were calculated for the notional destroyer modeled in the RTDS E-ship simulations. A ship displacement of 14,064 LT was obtained for a notional destroyer from [10]. The propeller diameter was set to 23 feet based on data in [7]. This is diameter was determined using a fixed pitch, 5 bladed, Wageningen B-Screw Series B5-75 propeller with a Pitch to Diameter (P/D) ratio of 1.4. The results of the calculations yielded a value of 2604 feet for the head reach and 106 seconds for the time-to-stop.

Running the E-ship model in speed control, with a maximum regenerative power limit of 2.7% (i.e., -1 MW), and a speed ramp rate of -10 percent per second, predicted a value of 2880 feet for head reach and 106 seconds for time-to-stop. Using these system characteristics, the results of the two models compare favorably. However, running the E-ship model with a maximum regenerative power limit of 11% (i.e., -4 MW) yields a head reach of 1680 feet and a time-to-stop of 63 seconds. It should be noted, therefore, that whereas the electrical power of the E-ship model's propulsion motors during regeneration was limited to a maximum value of 2.7%, motor power limitations implicit in the empirically-derived curves of the methodology by Crane, et. al. [1] were not available during this study.

IV. RTDS E-SHIP MODEL MOTOR CONTROL

Two forms of propulsion motor control are employed in the crashback simulations of the present paper. Their implementation in the RTDS E-ship model is illustrated in Figure 6. Both schemes are built on top of a current-control inner loop which controls the d-axis current to provide an appropriate flux level to the rotor and controls the q-axis current to achieve the requested torque. In the first form of control, a power control loop is employed to produce the torque reference; in the second, a speed control loop is used. In both cases, additional control features are required to successfully conduct the crashback maneuver.

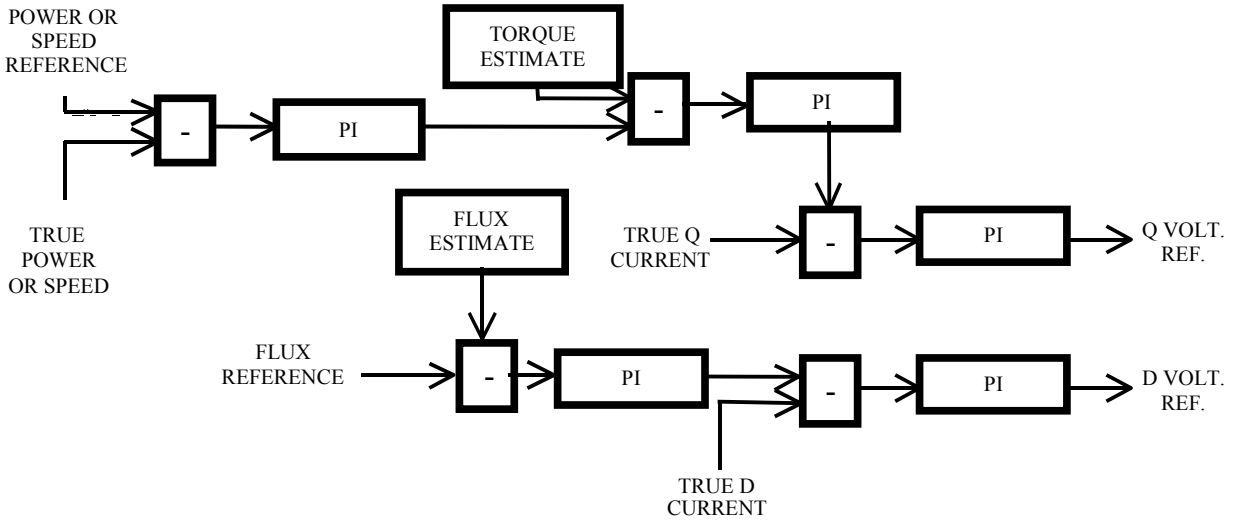

Figure 6. E-ship Model Propulsion Motor Controls

In the case of the power controller, the reference is passed through a ramp limiter, so the rate of change of the reference will not exceed the specified amount. There is also a limit on the level of regenerated power. When this limited is reached, as the ship's propellers slow down, the power ramp is halted and not resumed until the propellers can be slowed to zero without exceeding the regeneration limit. Finally, the sign of the power reference provided to the power controller is set so that the power requested from the motor is positive after propeller reversal has taken place, in spite of the fact the power requested by the operator is negative. The power specified by the operator may be thought of as the power "made good", in the sense that positive power is power expended moving the ship ahead and negative power is power expended to move the ship astern.

The speed control is also ramp limited and employs a supervisory higher-level control to ensure that the power stays below a maximum limit and above a regeneration limit. The supervisory control overrides the speed ramp, pausing it when a limit is reached and resuming it when the system can support the continued ramp. In addition, during Phase 3 of the crashback maneuver following the regeneration period, it was found to be necessary to actually back off the speed when the maximum power limit was reached in order to keep the limit from being exceeded. This is a consequence of the shape of the load power curve on the negative propeller-speed side, where the magnitude of the power increases, then decreases. The speed must be reduced briefly in order to pass over the peak without exceeding the maximum-power limit. This brief reduction in speed before the increase resumes may be seen in the results for both the speed and power control versions of the simulations presented later, and is a consequence of the physics embodied in the load power curve. An additional ramp override was originally incorporated that was triggered by excessive frequency excursions on the generator bus, but it primarily added noise to the system and failed to reduce the frequency variations.

The inner current-control loop employed in these controllers is a conventional PI system that has been used for basic speed-control of marine propulsion simulations at CAPS for a number of years (Woodruff [9]). D- and q-axis current-control loops produce corresponding voltage references that seek to keep the currents as close to reference current values as possible. The reference torque and flux are also produced by control loops, with the

feedback values produced by torque and flux estimators. The reference torque is produced by the speed or power controllers described above and the flux reference is set to an appropriate constant value. These intermediate torque and flux control loops are rarely used in practice in this type of application and could likely be eliminated from the present system without any significant loss of performance.

V. CRASHBACK SIMULATIONS

Simulations of IPS performance during a crash astern maneuver were performed by executing the RTDS E-ship model with the motor drive control scheme set first to operate in speed control mode, followed by runs in power control mode. Multiple runs were performed for each control mode by varying the initial ship velocity, the propulsion motor speed/power ramp rates, and the maximum level of permissible motor regenerative power.

The following indicators of IPS performance during the maneuver were evaluated:

1. Ship velocity,
2. Motor shaft speed,
3. Motor electrical power,
4. Motor electrical torque,
5. Main gas turbine generator power,
6. Main gas turbine generator frequency,
7. 800 VDC load center bus voltage,
8. Time to bring ship to full stop, and
9. The number of ship lengths to stop the ship.

The number of ship lengths required to reduce the ship velocity to zero (i.e., head reach in ship lengths) was calculated assuming a notional destroyer length of 600 feet [10].

Unless otherwise noted, it is assumed that the two main and two auxiliary generators are fully connected in a ring bus configuration, that 4 MW of ship's service load is distributed among the five zonal load centers, and that a 3 MW radar is operating.

1. Speed Control Simulations

Figure 7 shows the IPS dynamics with the propulsion motor drives operating in speed control. For this case, the ship was cruising at 30 knots with each propulsion motor rotating at 110.3 RPM. A crashback maneuver is initiated by requesting a motor speed of -110.3 RPM. The motor maximum regenerative power was limited to 11% (i.e., -4 MW) of its full 36.5 MW power rating. The speed ramp rate was fixed at -15% per second. The speed control supervisory controller described earlier limits the requested motor torque/power during the maneuver to a value greater than the maximum regenerative power limit and less than the motor's full power rating of 36.5 MW.

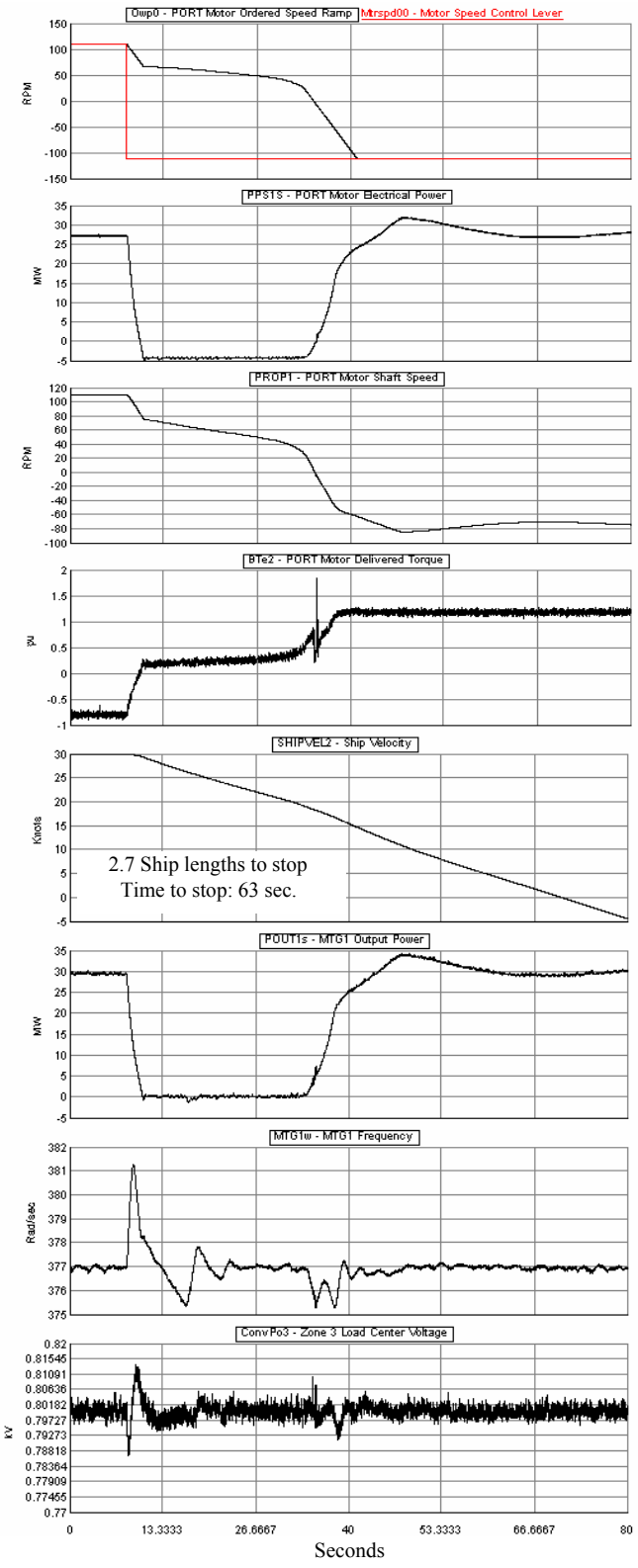

Figure 7. Speed Control Crashback Dynamics

The impact of performing such an extreme maneuver on the power distribution system is clearly seen by the plots of main generator 1's output power and frequency, as well as the 800 VDC bus voltage in Zone 3's load center. The generator frequency and bus voltage fluctuate at points of transition on the speed ramp curve.

The plots of Figures 8 through 11 show what happens when speed ramp rates of -5, -10, -21, and -22 percent per second are selected. Motor regenerative power is limited to -4 MW. As anticipated, the steeper the power ramp, the more quickly the ship comes to a full stop before reversing direction. This is evidenced by the decrease in number of ship lengths to stop from 3.2 to 2.7. In contrast, the magnitude of frequency and voltage fluctuations increase as ramp rate increases.

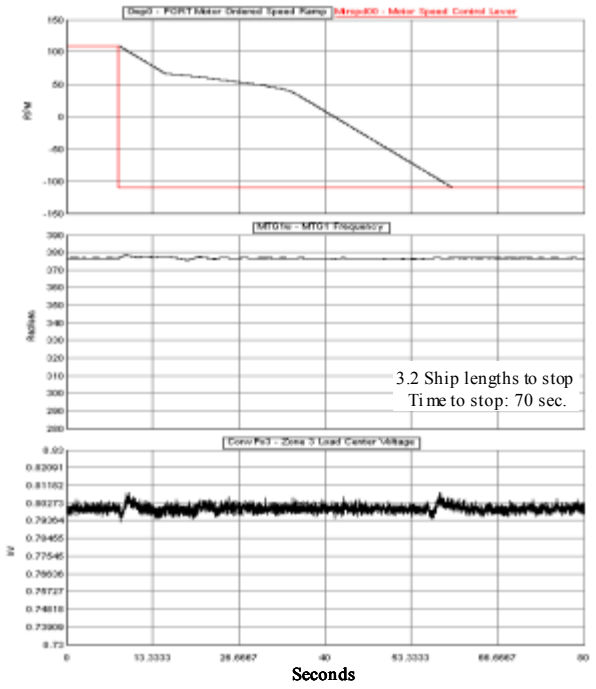

Figure 8. Speed Control Crashback: 5% per sec.

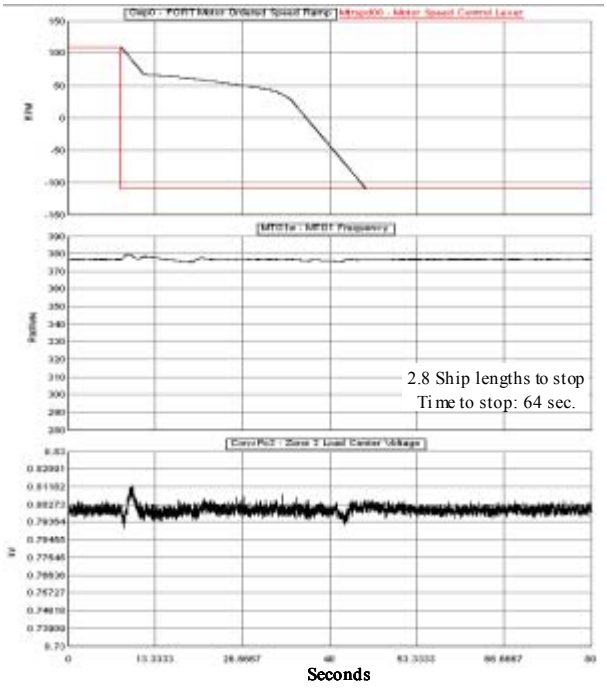

Figure 9. Speed Control Crashback: 10% per sec.

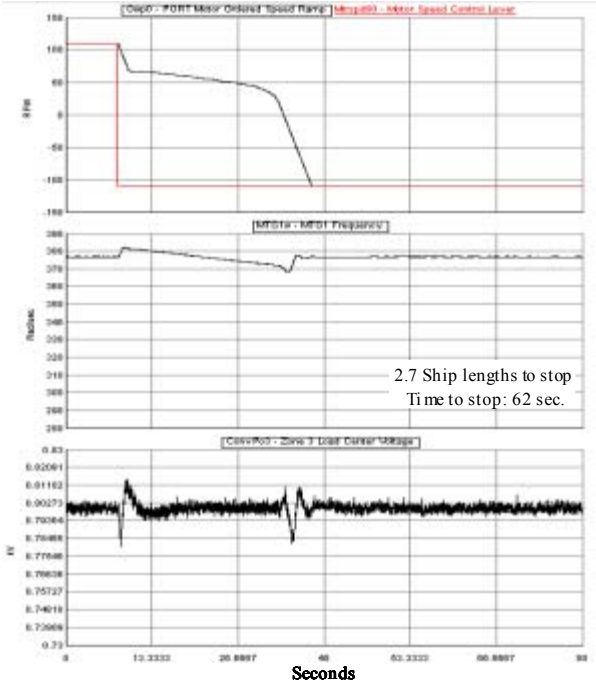

Figure 10. Speed Control Crashback: 21% per sec.

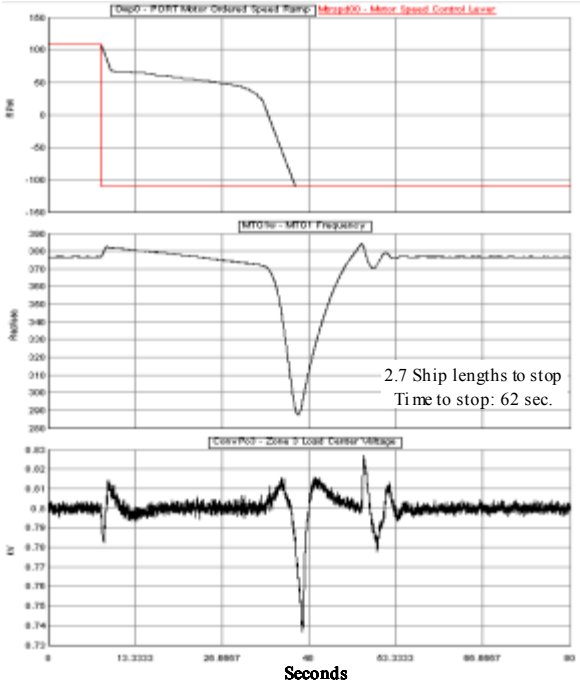

Figure 11. Speed Control Crashback: 22% per sec.

At a rate of -21% per sec., the frequency deviates from a nominal value of 376.99 rad/s by approximately 8 rad/s, or 2.1%. For a ramp rate of -22% per sec., the frequency excursion increases to 23.3%. MIL-STD-1399, Section 300A [11] specifies a maximum frequency transient tolerance for Type I (i.e., 60 Hz) shipboard power systems of +/- 4%. As a result, based on generator frequency, a practical ramp rate limit for the existing speed controller model is reached between -21 and -22 percent per second.

This study also explored IPS performance under different values of maximum permissible motor regenerative power while holding the speed ramp rate constant. Simulations were run with a speed ramp rate of -15% per second and regenerative power limits from -1 MW (i.e., 2.7%) to -5 MW (i.e., 13.7%) of 36.5 MW rated motor power. At present, the propulsion motor drives in the E-ship model employ fully regenerative front-ends. Instead of controlling motor regenerative power with braking resistors on the DC link, the power is passed on to the electrical distribution system supplying the motors. For this study, it is assumed that the gas turbine generators will not be required to dissipate power produced by the motors. Therefore, the maximum level of motor regenerative power is limited by the total ship load available to absorb the motor power produced during crashback. As a consequence, at the -5 MW regenerative power limit, the ship's service load was increased from 4 MW to 6 MW to avoid burdening the generators with regenerative power.

The slow downward drift of frequency during the regeneration cycle, seen clearly in Figures 10 and 11 (and later in power control crashback results), is a function of the controller design of the gas turbine model. Since the gas turbine is not required to dissipate regenerative power from the propulsion motors, the power output of this device is limited to positive values. Because of the extreme load rejection occurring during Phase 1 of the crashback power profile (i.e., from +26.75 MW to -4 MW), the power/torque requested from the gas turbines overshoots into negative values. During the periods of negative requested power/torque, the actual torque signal fed back to the synchronous generator model is limited to zero. The result is a slow downward drift of generator frequency. Improving the controller to minimize or eliminate overshoot in requested torque would avoid this condition. Improvements could also be achieved by allowing the gas turbines to function with the actual level of motor regenerative power specified by the gas turbine manufacturer.

Table 1 summarizes the principal parameter variations associated with different levels of maximum regenerative power. The changes in frequency or voltage excursions noted between the different levels of regeneration were insignificant. However, reducing the level of regeneration significantly reduces the duration of the maneuver and head reach.

Table 1. Speed Control Dynamics vs. Regeneration Level

Regenerative Power Limit, MW	Max. Frequency Fluctuation, %	Max. Voltage Fluctuation, %	No. of Ship Lengths to Stop	Time to Stop Ship, sec.
-1	+1.1/-0.5	+2.0/-1.6	4.8	106
-2	+1.1/-0.5	+2.0/-1.8	3.6	79
-3	+1.1/-0.6	+1.8/-1.3	3.1	69
-4	+1.1/-0.5	+1.8/-1.6	2.7	63
-5	+1.1/-0.7	-1.8/-1.8	2.5	59

Finally, this study explored the impact of different starting and ending ship speeds on IPS performance in speed control mode. Figure 12 shows the result of starting at 20 knots forward speed and requesting an ending speed of -30 knots (by requesting 110.3 RPM of motor speed). The maximum regenerative power level was -4 MW and the speed ramp rate was -15% per second. Predictably, the number of ship lengths to stop is reduced, from 2.7 to less than 1.1. Also, the disturbances in generator frequency and load bus voltage due to the downward ramp of motor power are reduced from +1.1/-0.4% to +0.5% frequency, and +1.6/-1.8% to +0.8/-1.3% voltage. However, the frequency and voltage fluctuations associated with reversing direction of the propellers are significantly larger, i.e., from -0.5% to -2.5% frequency deviation and -1.0% to -2.6% voltage deviation. Reducing the requested ending speed of the maneuver from -30 knots to -20 knots leaves the voltage fluctuation unchanged at -2.6%, but the frequency fluctuation is reduced slightly from -2.5% to -2.1%. This action also causes a slight increase in the time it takes to bring the ship to zero velocity from 41 to 43 seconds and the number of ship lengths to stop from 1.1 to 1.2.

2. Power Control Simulations

Figure 13 shows the IPS dynamics with the propulsion motor drives operating in power control mode. As with the speed control cases earlier, the ship was cruising at 30 knots with each propulsion motor consuming 26.75 MW of real power. A crashback maneuver is initiated by requesting a motor power of -26.75 MW. A power ramp rate of -15% per second was used and the motor maximum regenerative power was limited to -4 MW.

The plots of Figures 14 through 17 show system response to power ramp rates of -50, -100, -122, and -123 percent per second. As with speed control, increasing the power ramp rate increases the magnitude of disturbances in generator frequency and load voltage. When the +/- 4% frequency transient tolerance from MIL-STD-1399, Section 300A [11] is applied, as was done for speed control, a figure of 122% for maximum power ramp rate results.

Table 2 summarizes the principal parameter variations associated with different levels of maximum regenerative power. As with speed control, generator frequency and load voltage fluctuations do not change substantially with changes in regeneration level. However, the duration of the maneuver and the number of ship lengths to stop do reduce significantly with increasing regeneration level.

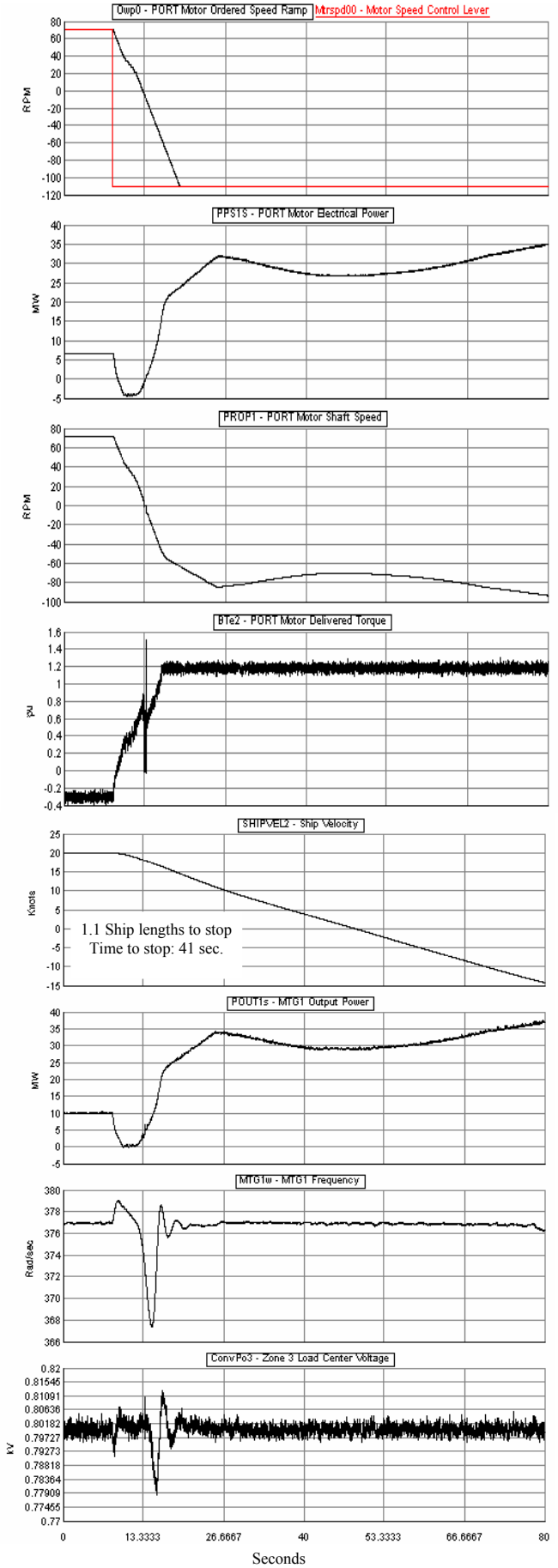

Figure 12. Speed Control Crashback: +20 knots to -30 knots

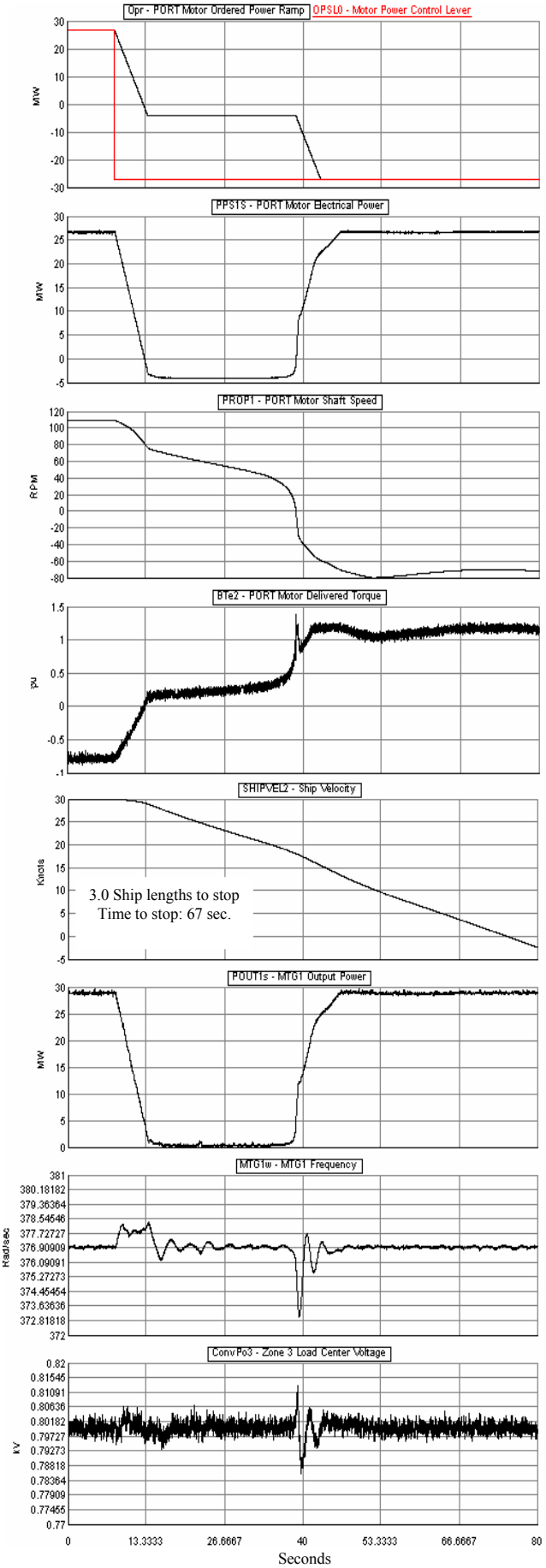

Figure 13. Power Control Crashback Dynamics

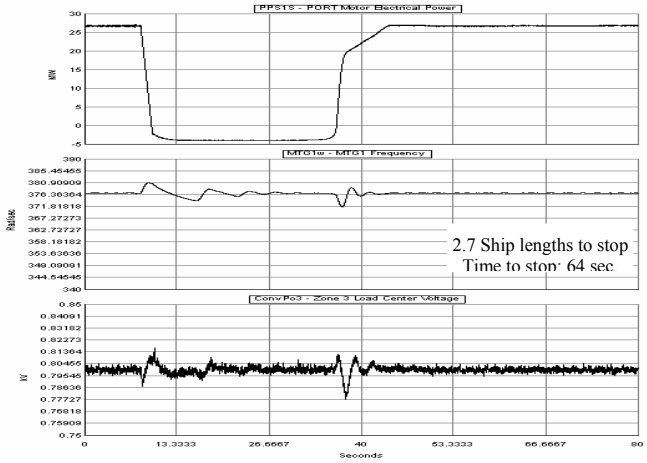

Figure 14. Power Control Crashback: 50% per sec.

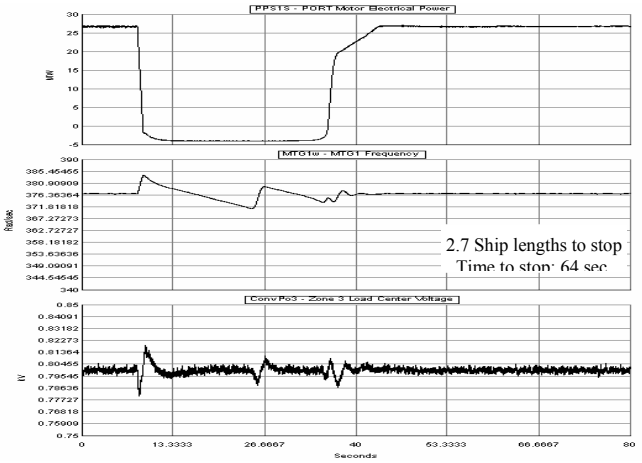

Figure 15. Power Control Crashback: 100% per sec.

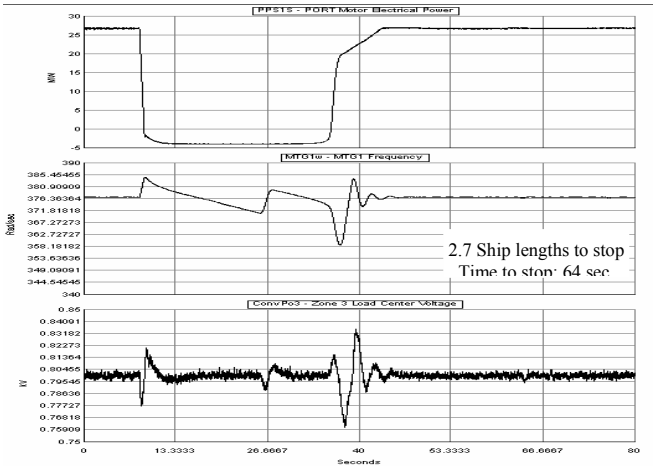

Figure 16. Power Control Crashback: 122% per sec.

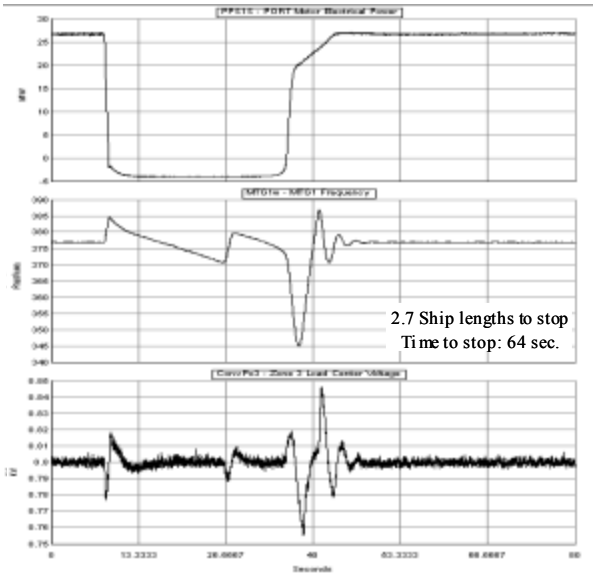

Figure 17. Power Control Crashback, 123% per sec.

Table 2. Power Control Dynamics vs. Regeneration Level

Regenerative Power Limit, MW	Max. Frequency Fluctuation, %	Max. Voltage Fluctuation, %	No. of Ship Lengths to Stop	Time to Stop Ship, sec.
-1	+0.3/-0.4	+1.0/-1.0	5.1	116
-2	+0.3/-0.5	+1.1/-0.9	4.0	87
-3	+0.3/-0.7	+1.1/-1.3	3.4	75
-4	+0.3/-1.0	+1.4/-1.5	3.0	67
-5	+1.1/-0.7	-1.8/-1.8	2.5	59

VI. CONCLUSIONS

The authors have examined the four phases of the crashback maneuver, identifying the critical limiting system characteristics in each phase and describing how generic power and speed controllers successfully control the system throughout the maneuver. Performing simulations of crashback with a detailed ship electrical model provided an opportunity to study the effects of the maneuver on the power distribution system, as well as the potential for the distribution-system dynamics to affect the propulsion-system performance. The simulations clearly predict expected increases in the magnitude of generator bus frequency and DC load center voltage fluctuations with increases in motor power and speed ramp rates. While the details of these results are naturally dependent on the particular design choices made for the notional ship system, the ability to predict both general trends and specific results for particular systems has been demonstrated. Such a capability might be used, for example, to make modifications to the motor controller in an attempt to moderate the generator-bus frequency excursions without significantly degrading crashback performance.

The results presented here highlight the critical role played by the maximum allowed regeneration level in determining the duration and head reach of a crashback maneuver. Adjustments in system controls that permit faster ramping of the power and propeller speed could reduce the maneuver duration by seconds and head reach by tenths of ship lengths. However, significantly greater performance improvement results from a larger

negative regenerative power limit. The ship designer seeking to meet crashback performance requirements should design schemes that optimize power and speed changes beyond what is possible with fixed ramp rates. However, he should not fail to explore any opportunity for increasing the maximum regeneration level. Even loads that are increased for a brief period in order to absorb regenerated power could be used to reduce the length of the regeneration phase of the crashback and permit full reverse thrust to be applied sooner.

The type of large-scale simulations reported here, particularly when combined with the hardware-in-the-loop experiments discussed by Ren, et. al. [6], provide a valuable tool for electric-ship researchers and designers. This paper shows how performance standards for shipboard power generation and distribution systems, such as AC bus frequency transient tolerance from MIL-STD-1399 [11], can be applied in designing motor drive controls for the crashback maneuver. With a lead time of years before electric-ship concepts can be tested at sea, these tools are vital for speeding propulsion- and power system development.

VII. ACKNOWLEDGEMENTS

The authors wish to gratefully acknowledge the support of the US Office of Naval Research, under grant No. N0014-02-1-0623, which made this work possible.

VIII. REFERENCES

[1] Chase, H.J., and Ad Hoc Panel Members, "Guide to the Selection of Backing Power," T. and R. Bulletin No. 3-5, SNAME, 1957.

[2] Crane, C. L., E. Haruzo, and A. C. Landsburg, "Controllability—Accelerating, Stopping and Backing", SNAME Principles of Naval Architecture Second Revision, Vol. III, Ed. by Edward V. Lewis, pp. 251-264, 1989.

[3] E. J. Lecourt, Jr., "Using Simulation to Determine the Maneuvering Performance of the WAGB-20," in *Naval Engineers Journal*, pp. 171-188, January 1998.

[4] Kuffel, R., J. Giesbrecht, T. Maguire, R.P. Wierckx, and P.G. McLaren, "RTDS-a fully digital power system simulator operating in real time:, in *Proc. of the WESCANEX 95., Comm., Power, and Computing*, IEEE, Vol. 2, 1995, pp. 300-305.

[5] Andrus, M., "RTDS Notional E-ship Model Technical Guide-Version 2.1a", *Internal Report*, CAPS, July 2006.

[6] Ren, W., M. Steurer, S. Woodruff, and M. Andrus, "Demonstrating the Power Hardware-in-the-Loop through Simulations of a Notional Destroyer-Class All-Electric Ship System During Crashback", in *Proc. of ASNE Advanced Propulsion Symposium*, Arlington, VA, Oct. 30-31 2006.

[7] Syntek, "DD(X) Notional Baseline Modeling and Simulation Development Report," *Internal Report*, August 2003.

[8] Syntek, "IPS Electric Plant One-line Diagram for a Notional Destroyer", *Internal Report*, August 2003.

[9] Woodruff, S., "Large-Scale Simulation of Naval Power Systems for Design Optimization", in *Proc. of EMTS*, Philadelphia, PA, January 27-29, 2004.

[10] Collins, M., "DD(X) Transformational Technologies for the Navy's Surface Combatant", in *Proc. of FIATECH*, Wilmington, DE, April 6-7, 2004.

[11] MIL-STD-1399 (NAVY), Section 300A, "Interface Standard for Shipboard Systems-Electric Power, Alternating Current", *NAVSEA*, Washington, DC, October 13, 1987.

IX. BIOGRAPHIES

Michael Andrus received a B.S.E.E. degree from Virginia Polytechnic Institute and State University in 1975. He is an Assistant Scholar Scientist at the Florida State University Center for Advanced Power Systems, where his work involves the large-scale modeling and simulation of shipboard power systems.

Stephen Woodruff received his Ph.D. in aerospace engineering from the University of Michigan. He is currently employed at the Florida State University Center for Advanced Power Systems, where he works on the development of simulation and hardware-in-the-loop techniques for power systems and their application to electric-ship systems.

Michael Steurer received a Master of Electrical Engineering in 1995 from the Vienna University of Technology, Austria, and his Ph.D. in Technical Science in 2001 from the Swiss Federal Institute of Technology Zurich, Switzerland, where he specialized in current limiting circuit breakers for the medium-voltage range. Dr. Steurer is currently a researcher at the Center for Advanced Power Systems at Florida State University (FSU) where he works primarily on hardware-in-the-loop real-time simulation and modeling of integrated power systems for all-electric ships. Dr. Steurer is a member of the IEEE and CIGRE and contributes to the CIGRE working group A3.16 "FCL impact on existing and new protection schemes" and the IEEE working group I8 "Power Electronic Building Blocks".

Wei Ren received the B.S. degree of Electrical Engineering in 1999 from the Shanghai Jiaotong University and is currently a Ph.D student of Electrical Engineering at Florida State University. He is working as a research assistant at the Center for Advanced Power Systems at Florida State University specializing in real time digital simulation.